RSC Advances

ROYAL SOCIETY OF CHEMISTRY

www.rsc.org/advances

Electrooxidation of the glycerol on the nickel and nickel alloys (Ni-Cu and Ni-Co) nanoparticles in alkaline media

Biuck Habibi*, Nasrin Delnavaz

Electroanalytical Chemistry Laboratory, Department of Chemistry, Faculty of Sciences, Azarbaijan Shahid Madani University, Tabriz, Iran

*Corresponding author (Biuck Habibi). E-mail: B.Habibi@azaruniv.edu, biuckhabibi_a@yahoo.com and Tel & Fax: +98-41 34327541

Abstract

In the present study, nickel (Ni) and Ni alloys (Ni-Cu and Ni-Co) nanoparticles modified carbon-ceramic electrodes (Ni/CCE, Ni-Cu/CCE and Ni-Co/CCE) were prepared by an electrochemical process. In order to obtain the surface and physicochemical information, the Ni/CCE, Ni-Cu/CCE and Ni-Co/CCE were investigated by scanning electron microscopy, energy dispersive X-ray spectroscopy, X-ray diffraction and electrochemical techniques. Then, the cyclic voltammetry and chronoamperometry were employed to characterize the electrocatalytic activity of the modified electrodes, Ni/CCE, Ni-Cu/CCE and Ni-Co/CCE, toward the oxidation of the glycerol in 1.0 M NaOH solution. It was found that the Ni alloys nanoparticles modified electrodes are catalytically more active than the Ni/CCE, therefore, the alloying of the Ni with Cu and Co in the form of nanoparticles on the carbon-ceramic electrode, as a homemade substrate, greatly enhances the catalytic activity of the Ni-based electrocatalysts (as the non-platinum electrocatalysts) in the glycerol oxidation.

Keywords: Glycerol, Electrooxidation, Nickel, Nickel-based alloys, Electrodeposition, Carbon-ceramic electrode.

1. Introduction

Metal and metal alloys nanoparticles due to their high specific surface area, reactivity, catalytic and electrocatalytic activities can be used extensively in many fields such as medicine, manufacturing and materials, environmental, energy and electronic [1-4]. Some of the use of these nanoparticles in energy field include: application in fuel cells, in solar energy systems, in batteries, in coal liquefaction and in transformers [5-9]. Among of the metal and metal alloys nanoparticles, Pt and Pt alloys due to unique chemical and physical characteristics have important applications in these areas especially in direct liquid fuel cells (DLFCs) [10, 11]. However, major barriers in the using, spreading and commercializing of the Pt and Pt alloy nanoparticles as electrocatalyst materials in DLFCs are the sluggish kinetics, poisoning by carbonaceous species and their high cost [12-13]. In practice, to solve these problems, the researchers have been focused on the alternative nanoparticles (non-platinum) with significant electrochemical activity as anodes or cathodes in DLFCs [14, 15]. The non-Pt-based nanoparticles are commonly used as electrocatalysts in fuel cells due to low cost, relatively abundant material and suitable catalytic activity [16-18]. Nickel (Ni) is one of the most commonly used non-Pt transition metals and is used to manufacture the electrocatalysts that are found in numerous electrochemical systems, such as rechargeable batteries, supercapacitors and fuel cells [19, 20]. In fuel cells field, there are few reports about the electrooxidation of alcohols such as methanol and ethanol on the Ni and Ni-based nanoparticles [21-25]. On the other hand, in order to improve the electrocatalytic performance of the Ni-based catalysts, bimetallic Ni such as Ni-Fe, Ni-Cu, Ni-Co, Ni-Cr and Ni-Mn have been investigated and reported [26-30].

Glycerol is a highly functionalized molecule containing three hydroxyl groups that are responsible for its solubility in water and its hygroscopic nature and is widely available from bio-sustainable sources and can be produced in a renewable, environmental-friendly, and cost-effective manner [31]. Glycerol would be promising in fuel cells because it is less toxic and inflammable, and also possess relatively high theoretical energy density. On the other hand, it is a good potential hydrogen source for fuel cells given a rapid growth of biodiesel production. The oxidation of glycerol has been systematically studied during the last recent years [32, 33] and few groups [29, 34-36] have been investigated and shown that the oxidation of glycerol proceeds on the Ni and Ni-based electrocatalysts.

In this work, the Ni and Ni-based alloys nanoparticles were electrodeposited on the carbon-ceramic electrode as a homemade substrate for the electrooxidation of the glycerol. The morphology, structure, composition and electrochemical behavior of the Ni and Ni-based alloys modified electrodes were characterized by scanning electron microscopy (SEM), energy dispersive X-ray spectroscopy (EDX), X-ray diffraction (XRD) and cyclic voltammetric methods, respectively. Then, the cyclic voltammetry and chronoamperometry approaches were employed to characterize the electrocatalytic activity of the present nanoparticles modified electrodes toward the oxidation of glycerol in 1.0 M NaOH solution. It was found that Ni-based alloys modified electrodes were electrocatalytically more active than Ni-alone nanoparticles modified electrode and had satisfactory stability and reproducibility when stored in ambient conditions or continues cycling.

2. Experimental

2.1. Chemicals

Methyltrimethoxysilane (MTMOS), glycerol, methanol, HCl, NaOH, H_2SO_4, Na_2SO_4, $NiCl_2.6H_2O$, $CoCl_2$, $CuCl_2.2H_2O$ and high purity graphite powder were obtained from Merck or Fluka. All solutions were prepared with double distilled water and all experiments were carried out at room temperature.

2.2. Instrumentation

The electrochemical experiments were carried out using an AUTOLABPGSTAT-30 (potentiostat/galvanostat) equipped with a USB electrochemical interface and driven GEPS software was used for electrochemical experiments. A conventional three electrode cell was used at room temperature. The modified electrodes (Ni/CCE, Ni-Cu/CCE and Ni-Co/CCE) (3 mm diameter) were used as the working electrode. A saturated calomel electrode (SCE) and a Pt wire were used as the reference and auxiliary electrodes, respectively. JULABO thermostat was used to control cell temperature at 25˚C. A scanning electron microscope (SEM), model LEO1430vp (Carl Zeiss, Germany) equipped with energy dispersive X-ray spectroscopy (EDX) was used to surfaces and surfaces chemical composition characterizations of the Ni, Ni-Cu and Ni-Co nanoparticles. X-ray diffraction of the nanoparticles was studied using a Bruker AXF (D8

Advance) X-ray power diffractometer with a Cu Kα radiation source (λ = 0.154056 nm) generated at 40 kV and 35 mA.

2.3. Preparation of the electrocatalysts

2.3.1. Preparation of the Ni/CCE

We have prepared the Ni nanoparticles modified CCE by a two-step procedure:

Step 1: The CCE, as a homemade substrate, was produced according to our previously works [33, 37, 38]. In briefly, the amount of 0.9 ml MTMOS was mixed with 0.6 ml methanol. After addition of 0.6 ml HCl 0.1 M as the catalyst, the mixture was magnetically stirred (for about 15 min) until producing a clear and homogeneous solution. Then, 0.3 g graphite powder was added and the mixture was stirred for other 5 minutes. Subsequently, the homogenized mixture was firmly packed into a Teflon tube (with 3 mm inner diameter and 10 mm length) and dried for at least 24 h at room temperature. A copper wire was inserted through the other end to set up electric contact. The electrode surface was polished with emery paper grade 1500 and rinsed with double distilled water.

Step 2: The Ni nanoparticles were electrodeposited on the obtained CCE in a 0.1 M Na_2SO_4, pH=3.4, continuous stirring solution containing 1 mM $NiCl_6.6H_2O$ at -0.6 V versus SCE for an optional time [39]. The charge resulting from the complete reduction of the Ni ions at the given time is 2385 mC/cm^2. This value corresponds to 0.725 mg/cm^2 of the Ni on the CCE. The Ni/CCE was washed thoroughly with double distilled water and dried before further investigations.

2.3.2. Preparation of the Ni-Cu/CCE and Ni-Co/CCE

The CCE was prepared according to the above mentioned method. The Ni-Cu and Ni-Co alloys nanoparticles on the CCE were electrodeposited (potentiostatically) from the aqueous solutions of 0.1 M Na_2SO_4 pH=3.4 comprising 1:1 ratio of $NiCl_6.6H_2O$ and $CuCl_2.2H_2O$ for Ni-Cu alloy deposition and 1.5:0.5 ratio of $NiCl_6.6H_2O$ and $CoCl_2$ for Ni-Co alloy nanoparticles (total concentration of two salts equal to 2 mM) at -0.6 V versus the SCE for a certain time. The mass values of alloys nanoparticles electrodeposited on the surface of the CCE are corresponding to an equivalent amount of Ni similar to Ni/CCE if Ni is considered as the only metal electrodeposited.

3. Results and discussion

3.1. Physicochemical characterization of the Ni/CCE, Ni-Cu/CCE and Ni-Co/CCE

In order to characterize the surface morphology of the present modified electrodes, the surface of the Ni/CCE, Ni-Cu/CCE and Ni-Co/CCE was investigated by SEM and corresponding images were shown in Fig. 1. Fig. 1(A) displays the image of the CCE after Ni nanoparticles electrodeposition. This image reveals a high density of globular particles of the Ni nanoparticles with different sizes. The globular like structure of Ni nanoparticles probably are not the individual Ni crystallites. Undoubtedly, they are collections, like as a globular, consisting of crystallite aggregates. Fig. 1(B) shows the SEM image of Ni-Cu/CCE. As can be seen, the surface of the Ni-Cu/CCE is completely different with respect to Ni/CCE surface. This image shows the hierarchical structures with dendritic morphology (with high magnification in Fig. 1C) [40, 41]. Fig. 1(D) displays the SEM image of the CCE after Ni-Co alloy electrodeposition. The Ni-Co alloy with spherical structure and high density formed on the CCE. Its surface investigation shows that the Ni-Co nanoparticles have the size of 30-80 nm. It seems that, each spherical like structures of Ni-Co is not the individual Ni-Co crystallites [42]. The surface chemical composition of the Ni/CCE, Ni-Cu/CCE and Ni-Co/CCE was investigated by EDX analysis (Fig. 2). The EDX spectrum of Ni/CCE (Fig. 2A) contains strong peaks at approximately 0.8, 7.5, 8.2 KeV for Ni element, suggesting that the single Ni nanoparticles are electrodeposited on the CCE [42]. The EDX analysis of the Ni-Cu/CCE (Fig. 2B) and Ni-Co/CCE (Fig. 2C) reveals the presence of the Ni, Co and Cu atoms. On the other hand, the presence and distribution of the two components (Ni and Cu in the case of Ni-Cu/CCE and Ni and Co in the case of Ni-Co/CCE) registered by the EDX analysis [41, 42]. In all spectra in Fig. 2, the peaks at about 0.4, 0.7 and 1.9 keV correspond to Si, O and C atoms, respectively, which attributed to the CCE structure.

To characterize the crystal structure of the present modified electrodes, the XRD experiment was used. Fig. 3 shows the XRD patterns of the Ni/CCE, Ni-Cu/CCE and Ni-Co/CCE. In all XRD patterns, the peak at 2θ of 55° corresponds to carbon (006) of the support material (carbon-ceramic). The main peaks in the XRD pattern of the Ni/CCE (A) at 2θ values of 42.6°, 43.6°, 44.76°, 46.41°, 52°, 60.15° and 77.71° corresponding to (010), (002), (111), (011), (200), (012) and (220) crystal planes for Ni, respectively. Using the Scherrer equation [37]; D_c=

0.9 λ/β cos θ (where λ= 0.154056 nm, β is the full width at half-maximum in radians and θ is the peak position in degrees), the average crystallite size (D_c) of Ni nanoparticles form the 2θ at the 44.76° (111) is estimated to be about 24 nm. In XRD patterns of the Ni-Cu/CCE (B) and Ni-Co/CCE (C), the strong diffraction peaks at 2θ values of 42.6°, 43.6°, 44.76°, 46.41°, 51°, 60.15° and 77.71° corresponding to (010), (002), (111), (011), (200), (012) and (220) for pure Ni, pure Cu or Ni-Cu alloy in the case of the Ni-Cu/CCE and pure Ni, pure Co or Ni-Co alloy in Ni-Co/CCE, respectively [41, 43]. As can be seen, the XRD pattern of Ni/CCE and also the Ni-Cu/CCE and Ni-Co/CCE are almost similar because these elements have successive atomic number, close atomic weight and same crystal structure in the normal conditions [44, 45].

For the electrochemical characterization of the Ni/CCE, Ni-Cu/CCE and Ni-Co/CCE electrocatalysts the cyclic voltammetric studies were used. Fig. 4 shows the cyclic voltammograms (CVs) of the Ni/CCE, Ni-Cu/CCE and Ni-Co/CCE electrocatalysts recorded in the supporting electrolyte at a scan rate 50 mV s^{-1} ; 1.0 mol L^{-1} NaOH solution. As can be seen in Fig. 4 (A), during the forward scan, after a double layer region in the range of -1.0 to +0.3 V vs. SCE, an anodic peak appears at about +0.4 V (wave a_1), where the surface of the Ni/CCE is mainly covered by Ni hydroxides and then the characteristic behavior assigned to redox couple of Ni(II)/Ni(III): [$Ni(OH)_2 + OH^- \leftrightarrow NiOOH + H_2O + e^-$] happens in higher potential region (from 0.6 to 1.0 V) prior to the oxygen evolution reaction. During the reverse scan, a cathodic peak at about +0.25 V (wave a'_1), corresponds the a_1 anodic peak [$Ni + 2OH^- \leftrightarrow Ni(OH)_2 + 2e^-$] and also a small cathodic peak at about -0.6 V (wave D_1) occur, represents the existence of different phases of Ni oxides on the Ni/CCE surface. On the other hand, the later cathodic peak, D_1, could possibly be due to the discharge of the γ-NiOOH phase to α or β-$Ni(OH)_2$ obtained during the charging of β-$Ni(OH)_2$ or partially overcharging of the β-NiOOH [46, 47]. The electrochemical behavior of Ni electrode in alkaline medium has been reported previously [48-52]. Comparison the reported results in the literature with our results shows a good agreement between them. Based on the stated results, Ni electrode is oxidized to a highly hydrated α-$Ni(OH)_2$ according to: $Ni + 2OH^- \leftrightarrow Ni(OH)_2 + 2e^-$, at the lower potentials in the first scan of cyclic voltammetry studies and the resulted hydroxides [α-$Ni(OH)_2$] cover the electrode surface. The electrooxidation of Ni to α-$Ni(OH)_2$ is a reversible process; wave a_1 and a'_1 in Fig. 4(A). With increasing the potential in the positive direction the α-$Ni(OH)_2$ convert to the β-$Ni(OH)_2$,

which is more stable and less hydrated than α-$Ni(OH)_2$, via an irreversible process. So that the conversion of β-$Ni(OH)_2$ to α-$Ni(OH)_2$ and also to atomic Ni is not possible. At the more positive potentials, the β-$Ni(OH)_2$ converted to NiOOH [23, 30, 34, 51-53].

Fig. 4(B) shows the CV of the Ni-Cu/CCE in the same supporting electrolyte. Besides the anodic (wave a_2) and cathodic (wave a'_2) peaks in the CV of the Ni-Cu/CCE, there are two other anodic peaks, A_1 and A_2, from -0.6 to 0.0 V and one cathodic peak, C_1, at the about -0.9 V correspond to the following reactions [54-57]:

$Cu + OH^- \rightarrow Cu(OH) + e^-$: wave A_1

$Cu(OH) + OH^- \rightarrow CuO + H_2O + e^-$: wave A_2

$CuO + H_2O + e^- \rightarrow Cu(OH) + OH^-$ or $2CuO + H_2O + 2e^- \rightarrow Cu_2O + 2OH^-$: wave C_1

and also some cumulative effects of the presence of the Cu atoms on the anodic and cathodic peak currents of Ni system. So that, the anodic and cathodic peak currents of Ni oxidation and reduction on the Ni-Cu/CCE were increased two orders with respect to Ni/CCE [Fig. 4(A)]. Therefore the surface oxides layer on the Ni-Cu alloy nanoparticles modified electrode is subsequently transformed to a mixture of NiOOH and CuO or Cu(OH). Also, according to the literature [57-58], some of the Cu(OH) and CuO can be oxidized further to the Cu^{3+} oxide in high potentials prior to the oxygen evolution reaction.

While the Ni-Co/CCE electrocatalyst in supporting electrolyte exhibits a CV [Fig. 4 (C)] that is very similar to the CV of the Ni/CCE in the same electrolyte. However, some differences, especially in the peak currents and potential region of the redox couple of the $Ni + 2OH^- \leftrightarrow Ni(OH)_2 + 2e^-$, appear on it. The presence of Co atoms in the electrocatalyst structure changes the peak currents and peak potentials; the anodic peak current (wave a_3) and corresponding cathodic peak current (wave a'_3) in CV of the Ni-Co/CCE ($I_{wave\ a3}$=1.8 mA) are higher than that of the Ni/CCE [$I_{wave\ a1}$=0.5 mA in Fig. 4(A)] with sharp appearances and in less positive potentials. Also, in the reverse scan the cathodic peak (wave D_3) was increased more than two orders with respect to Ni/CCE, indicating the existence of different phases of Ni and Co oxides on the Ni-Co/CCE surface. These changes in the CV profile of the Ni-Co/CCE are probably due to the formation of $Co(OH)_2$ from the corresponding Co atoms that occurs earlier than that of $Ni(OH)_2$. It is reported that the addition of Cu or Co to Ni particles such as Ni-Cu or Ni-Co alloys modified electrodes or even other metals such as Cd, Zn, Ca and Ti elements as solid solutes to

the Ni, represents a very efficient strategy of suppressing the formation of the β-NiOOH phase [47, 56-58]. Therefore, the electrochemical behavior of the pure electrodeposited Ni and Ni-Cu and Ni-Co alloy modified electrodes reveals good stabilization of the β oxyhydroxide form on the alloy nanoparticles and the effects of this phenomenon obviously appearance on the CV profiles of the Ni-Cu and Ni-Co alloy modified electrodes [47].

3.2. Electrocatalytic activity of the Ni/CCE, Ni-Cu/CCE and Ni-Co/CCE

Fig. 5 shows the CVs of the Ni/CCE, Ni-Cu/CCE and Ni-Co/CCE electrocatalysts in the absence and presence of the glycerol in alkaline solution. Red lines in Fig. 5 display the CVs of Ni/CCE, Ni-Cu/CCE and Ni-Co/CCE in 1.0 M NaOH solution containing 0.1 M glycerol at a scan rate 50 mV s^{-1}. As can be seen in the CVs of the Ni/CCE (A), Ni-Cu/CCE (B) and Ni-Co/CCE (C), the oxidation reaction of glycerol has the same appearance and starts concomitantly with the formation of the $Ni/Ni(OH)_2$ on the Ni/CCE (Fig. 5A) and corresponding peaks at the alloy nanoparticles on the Ni-Cu/CCE (Fig. 5B) and Ni-Co/CCE (Fig. 5C). The electrooxidation of glycerol commences (onset oxidation potential) at about 0.4V, 0.3V and 0.219 V vs. SCE on the Ni/CCE, Ni-Cu/CCE and Ni-Co/CCE electrocatalysts, respectively. At potentials more than ca. 0.4V on the Ni/CCE, 0.3V on the Ni-Cu/CCE and 0.219 V on the Ni-Co/CCE, the reaction becomes accelerated and maximum currents occur at ca. 0.79 V (Ni/CCE), 0.72 V (Ni-Cu/CCE) and 0.55V (Ni-Co/CCE), respectively. The performance of the present electrocatalysts toward the oxidation of the glycerol was evaluated by three parameters: (1) onset oxidation potential, (2) forward anodic peak potential and (3) forward anodic peak current. These electrochemical parameters in the glycerol oxidation at the Ni/CCE, Ni-Cu/CCE and Ni-Co/CCE electrocatalysts are listed in Table 1. As can be seen in Table 1, the lower onset oxidation potential, forward anodic peak potential and higher anodic peak current for Ni-based alloys disclose that the Ni-based alloys have the high electrocatalytic activity toward the glycerol oxidation with respect to alone Ni modified electrode (Ni/CCE). As mentioned above, due to the higher surface concentration of the β-NiOOH form in the Ni-Cu/CCE and Ni-Co/CCE because of the presence of the Cu and Co, the alloy modified electrodes generate a higher electrocatalytic activity toward glycerol oxidation in NaOH solution with respect to Ni/CCE. On the other hand, comparison of the black lines (absence of glycerol) and red lines (presence of glycerol) in Fig. 5 shows that the oxygen evolution reaction occurs at more positive potentials when glycerol is present in NaOH

solution. As reported in the literature [59], this may be due to a higher adsorption affinity of elevated valence Ni or mixed Ni-Cu and N-Co intermediate species for glycerol than for hydroxyl species (OH^-). Alternatively, in presence of glycerol (red lines) the cathodic peaks originally observed in the absence of glycerol (black lines) (a'_1, a'_2 and a'_3 and also D_1) during the revers scan disappear completely. These effects could be associated to the dependency of the beginning of the glycerol oxidation with the preliminary steps of the transformation of $Ni(OH)_2$ to NiOOH at the surface of electrocatalysts [60]. Therefore, these results indicate that the Ni-based electrocatalysts can catalyze the glycerol oxidation in alkaline media; where the possible intermediates and final products including glyceraldehyde, dihydroxyacetone and carboxylic compounds such as glyceric, glycolic, formic, tartronic, hydroxypyruvic, oxalic, and ketomalonic acids are formed from the glycerol electrooxidation (scheme 1)[61-62]. As can be seen in scheme 1, the glycerol oxidation is made up of complex pathway reactions that can produce a large number of useful intermediates or valuable fine chemicals along with the exchange of electrons [63].

In order to determine of kinetic parameters of the electrooxidation of glycerol at the Ni/CCE, Ni-Cu/CCE and Ni-Co/CCE, the Tafel analysis was planned. Fig .6 shows the Tafel plots resulted from the CVs of 0.1 M glycerol in 1.0 M NaOH solution on the Ni/CCE (A), Ni-Cu/CCE (B) and Ni-Co/CCE (C) at a scan rate of 20 mV s^{-1}. The slope of Tafel plots are 253, 245 and 175 mV dec^{-1} for glycerol electrooxidation at the Ni/CCE, Ni-Cu/CCE and Ni-Co/CCE, respectively. The αn_α values can be calculated from the Butler-Volmer equation [64, 65]: Log i = Log i_o+ αn_α Fη/2.303 RT; the constants R and F denote the universal gas constant and the Faraday constant, respectively, T is the temperature (in K), α is the charge transfer coefficient of the reaction, i_o is the exchange current density, n_α is the number of electrons transferred in the rate-determining step and η is the overpotential. The αn_α evaluated from the slope of Tafel plots, are 0.23, 0.24 and 0.34 for glycerol electrooxidation at the Ni/CCE, Ni-Cu/CCE and Ni-Co/CCE, respectively. In the electrochemical oxidation of glycerol, the rate-determining step is a one-electron process [29, 30], n_α=1; thus, α values should be 0.23, 0.24 and 0.34 for glycerol electrooxidation at the Ni/CCE, Ni-Cu/CCE and Ni-Co/CCE, respectively.

The effect of scan rate on the electrooxidation of glycerol at the Ni/CCE, Ni-Cu/CCE and Ni-Co/CCE was done and results were shown in Fig. 7(A), (B) and (C), respectively. As can be

seen, the anodic peak currents in all cases increase with the scan rate. The relation between the anodic peak currents of glycerol oxidation obtained in forward scan and square root of scan rates ($v^{1/2}$) are shown in the insets of Fig. 7 A, B and C (I for the Ni/CCE, I' for Ni-Cu/CCE and I'' for Ni-Co/CCE). The anodic peak currents are linearly proportional to the square root of scan rates, which indicate the electrocatalytic oxidation of glycerol at the Ni/CCE (A), Ni-Cu/CCE (B) and Ni-Co/CCE (C) may be controlled by a diffusion process. In addition, the peak potentials of the oxidation of glycerol at the Ni/CCE, Ni-Cu/CCE and Ni-Co/CCE shift to high potentials with increasing of the scan rate (insets of II (A), II' (B) and II'' (C) in Fig. 7 for the Ni/CCE, Ni-Cu/CCE and Ni-Co/CCE, respectively). These results indicate that the electrooxidation of glycerol at the Ni/CCE, Ni-Cu/CCE and Ni-Co/CCE is an irreversible electrode process.

3.3. Long-term stability of the Ni/CCE, Ni-Cu/CCE and Ni-Co/CCE

In view of practical applications, long-term stability of the electrocatalysts is important. The long-term stability of the Ni/CCE, Ni-Cu/CCE and Ni-Co/CCE was firstly examined in 1.0 M NaOH containing 0.1 M glycerol by cyclic voltammetry. The obtained results indicate that the anodic peak currents in the forward scan remain constant with an increase in scan numbers at the initial stage and then start to decrease after 30 scans. The peak currents of the 500th scan are about between 93-95% than that of the first scan for the electrocatalysts (not shown here). In general, the loss of the catalytic activity after successive number of scans may result from the consumption of glycerol during the CV scan. It may also be due to poisoning and the structure change of the Ni and Ni-based nanoparticles as a result of the perturbation of the potentials during the scanning in aqueous solutions, especially in presence of the organic compound. Another factor might be due to the diffusion process occurring between the surface of the electrocatalysts and the bulk solution. With an increase in scan numbers, glycerol molecules diffuse gradually from the bulk solution to the surface of the electrocatalysts. After the long-term CV experiments, the present electrocatalysts were stored in water for a week; then glycerol oxidation was carried out again by CV, and excellent catalytic activities toward glycerol oxidation were still observed on the Ni/CCE, Ni-Cu/CCE and Ni-Co/CCE electrocatalysts. In order to further evaluation the stability of the electrocatalytic activity of the Ni/CCE, Ni-Cu/CCE and Ni-Co/CCE toward glycerol oxidation, chronoamperometric measurements were performed by applying two different applied potentials for 700s. Fig. 8 displays the chronoamperometric

curves of 0.1 M glycerol oxidation in 1.0 M NaOH at the Ni/CCE (A), Ni-Cu/CCE (B) and Ni-Co/CCE (C) under constant potentials of (0.6 V and 0.8 V) for Ni/CCE, (0.6 V and 0.75 V) for Ni-Cu/CCE and (0.4 V and 0.55 V) for Ni-Co/CCE electrocatalysts. It was found that the currents observed from chronoamperograms were in good agreement with the currents observed from cyclic voltammetry. These results indicate that the present electrocatalysts have good long-term stability and storage properties.

4. Conclusions

A simple electrochemical method was used to fabricate the Ni and Ni alloys (Ni-Cu and Ni-Co) nanoparticles on the carbon-ceramic electrode as the electrocatalysts for the oxidation of glycerol. The prepared modified electrodes, Ni/CCE, Ni-Cu/CCE and Ni-Co/CCE, were characterized by XRD, SEM, EDX and electrochemical techniques. The SEM studies show the well-dispersed and spherical nanoparticles of the Ni and Ni-Co alloy on the CCE; the size of these nanoparticles were about 24 nm for alone Ni and between 30-80 nm for the Ni-Co alloy, respectively. While, the Ni-Cu alloy nanoparticles were electrodeposited on the CCE as the hierarchical structures with dendritic morphology. The EDX analyses confirm the presence of the alone Ni and its alloy in the Ni/CCE, Ni-Cu/CCE and Ni-Co/CCE, respectively. On the other hand, the XRD patterns show that the Ni/CCE, Ni-Cu/CCE and Ni-Co/CCE display the characteristic diffraction peaks of a face-centered cubic Ni structure. The cyclic voltammetric and chronoamperometric studies reveal that the Ni/CCE, Ni-Cu/CCE and Ni-Co/CCE have high electrocatalytic activities toward the oxidation of glycerol. The obtained results show that, relative to alone Ni, Ni-based alloys nanoparticles modified electrodes exhibit a greatly enhanced performance in terms of the low onset potential, higher anodic peak current and low positive peak potential in the electrooxidation of glycerol. Therefore the Ni-based alloy nanoparticles on the carbon-ceramic electrode are the promising electrocatalysts for the oxidation of glycerol in alkaline media.

Acknowledgment

The authors gratefully acknowledge the research council of Azarbaijan Shahid Madani University for financial support.

References:

[1] Bashyam R, Zelenay P. A class of non-precious metal composite catalysts for fuel cells. Nature 2006;443:63-66.

[2] Chan KY, Ding J, Ren J, Cheng S, Tsang KY. Supported mixed metal nanoparticles as electrocatalysts in low temperature fuel cells. J Mater Chem 2004;14:505-516.

[3] You H, Yang S, Ding B, Yang H. Synthesis of colloidal metal and metal alloy nanoparticles for electrochemical energy applications. Chem Soc Rev 2013;42:2880-2904.

[4] Stamenkovic VR, Mun BS, Arenz M, Mayrhofer KJJ, Lucas CA, Wang G, Ross PN, Markovic NM. Trends in electrocatalysis on extended and nanoscale Pt-bimetallic alloy surfaces. Nature Materials 2007;6:241-247.

[5] Matsui I. Nanoparticles for electronic device applications: a brief review. J Chem Eng Jpn 2005;38:535-546.

[6] Lue JT. A review of characterization and physical property studies of metallic nanoparticles. J Phys Chem Solids 2001;62:1599-1612.

[7] Kittelson DB. Engines and nanoparticles: a review. J Aerosol Sci 1998;29:575-588.

[8] Gambhire VM, Gambhire MS, Bhatt SM, Jain KS. Nanoparticles in drug targeting-a review. Indian Drugs 2010;47:5-18.

[9] Kane J, Ong J, Saraf RF. Chemistry, physics, and engineering of electrically percolating arrays of nanoparticles: a mini review. J Mater Chem 2011;21:16846-16858.

[10] Sheikh AM, Ebn-Alwaled AAK, Malfatti CF. On reviewing the catalyst materials for direct alcohol fuel cells (DAFCs). J Multidisciplinary Engineering Science and Technology (JMEST) 2014;1:1-9.

[11] Liu H, Song C, Zhang L, Zhang J, Wang H, Wilkinson DP. A review of anode catalysis in the direct methanol fuel cell. J Power Sources 2006;155:95-110.

[12] Jingyu S, Jianshu H, Yanxia C, Xiaogang Z. Hydrothermal synthesis of Pt-Ru/MWCNTs and its electrocatalytic properties for oxidation of methanol. Int J Electrochem Sci 2007;2:64-71.

[13] Witham CK, Chun W, Valdez TI, Narayanan SR. Performance of direct methanol fuel cells with sputter-deposited anode catalyst layers. Electrochem Solid State Lett 2000;3:497-500.

[14] Brouzgou A, Song SQ, Tsiakaras P. Low and non-platinum electrocatalysts for PEMFCs: Current status, challenges and prospects. Appl Catal B: Environmental 2012;127:371-388.

[15] Serov A, Kwak C. Review of non-platinum anode catalysts for DMFC and PEMFC application. Appl Catal B: Environmental 2009;90:313-320.

[16] Wang B. Recent development of non-platinum catalysts for oxygen reduction reaction. J Power Sources 2005;152:1-15.

[17] Serov A, Kwak C. Review of non-platinum anode catalysts for DMFC and PEMFC application. Appl Catal B: Environmental 2009;90:313-320.

[18] Bashyam R, Zelenay P. A class of non-precious metal composite catalysts for fuel cells. Nature 2006;443:63-66.

[19] Amjad M, Pletcher D, Smith C. The Oxidation of Alcohols at a Nickel Anode in Alkaline t-Butanol/Water Mixtures. J Electrochem Soc 1977;124:203-206.

[20] Gong M, Dai H. A mini review of NiFe-based materials as highly active oxygen evolution reaction electrocatalysts. Nano Research 2015;8:23-39.

[21] Abdel Rahim MA, Abdel Hameed RM, Khalil MW. Nickel as a catalyst for the electro-oxidation of methanol in alkaline medium. J Power Sources 2004;134:160-169.

[22] Gabaly FE, McCarty KF, Bluhm H, McDaniel AH. Oxidation stages of Ni electrodes in solid oxide fuel cell environments. Phys Chem Chem Phys 2013;15:8334-8341.

[23] Jin GP, Ding YF, Zheng PP. Electrodeposition of nickel nanoparticles on functional MWCNT surfaces for ethanol oxidation. J Power Sources 2007;166:80-86.

[24] Fleischmann M, Korinek K, Pletcher D. The oxidation of organic compounds at a nickel anode in alkaline solution. J Electroanal Chem Interfacial Electrochem 1971;31:39-49.

[25] Nelson R. Stradiotto, Kathryn E. Toghill, Lei Xiao, Amir Moshar, Richard G. Comptonb. The Fabrication and Characterization of a Nickel Nanoparticle Modified Boron Doped Diamond Electrode for Electrocatalysis of Primary Alcohol Oxidation. Electroanalysis 2009;21:2627-2633.

[26] Danaee I, Jafarian M, Mirzapoor A, Gobal F, Mahjani MG. Electrooxidation of methanol on NiMn alloy modified graphite electrode. Electrochim Acta 2010;55:2093-100.

[27] Marioli JM, Luo PF, Kuwana T. Nickel-chromium alloy electrode as a carbohydrate detector for liquid chromatography. Anal Chim Acta 1993;282:571-80.

[28] Forouzandeh F, Danaee I, Gobal F, Mahjani MG. Electrocatalytic oxidation of glucose on Ni and NiCu alloy modified glassy carbon electrode. J Solid State Electrochem 2008;13:1171-1179.

[29] Oliveira VL, Morais C, Servat K, Napporn TW, Tremiliosi-Filho G, Kokoh K.B. Glycerol oxidation on nickel based nanocatalysts in alkaline medium - Identification of the reaction products. J Electroanal Chem 2013;703:56-62.

[30] Oliveira VL, Morais C, Servat K, Napporn TW, Tremiliosi-Filho G, Kokoh KB. Studies of the reaction products resulted from glycerol electrooxidation on Ni-based materials in alkaline medium. Electrochim Acta 2014;117:255-262.

[31] Xuan J, Leung MKH, Leung DYC, Ni M, Sust R. A review of biomass-derived fuel processors for fuel cell systems. Energy Rev 2009;13:1301-1313.

[32] Kim HJ, Choi SM, Green S, Tompsett GA, Lee SH, Huber GW, Kim WB. Highly active and stable PtRuSn/C catalyst for electrooxidations of ethylene glycol and glycerol. Appl Catal B: Environmental 2011;101:366-375.

[33] Habibi B, Ghaderi S. Synthesis, characterization and electrocatalytic activity of Co@Pt nanoparticles supported on carbon-ceramic substrate for fuel cell applications. Int J Hydrogen Energy 2015;40:5115-6125.

[34] Faro M Lo, Minutoli M, Monforte G, V Antonucci, Aricò AS. Glycerol oxidation in solid oxide fuel cells based on a Ni-perovskite electrocatalyst. Biomass Bioenerg 2011;35:1075-1084.

[35] Oliveira VL, Morais C, Servat K, Napporn TW, Tremiliosi-Filho G, Kokoh KB. Studies of the reaction products resulted from glycerol electrooxidation on Ni-based materials in alkaline medium. Electrochim Acta 2014;117:255-262.

[36] Kannan R, Karunakaran K, Vasanthkumar S. PdNi-decorated manganite nanocatalyst for electrooxidation of ethylene glycol in alkaline media. Ionics 2012;18:803-809.

[37] Habibi B, Delnavaz N. Electrocatalytic oxidation of formic acid and formaldehyde on platinum nanoparticles decorated carbon-ceramic substrate. Int J Hydrogen Energy 2010;35: 8831.

[38] Habibi B, Mohammadyari S. Facile synthesis of Pd nanoparticles on nano carbon supports and their application as an electrocatalyst for oxidation of ethanol in alkaline media: The effect of support. Int J Hydrogen Energy 2015;40:10833-10846.

[39] Habibi B, Gahramanzadeh R. Fabrication and characterization of non-platinum electrocatalyst for methanol oxidation in alkaline medium: Nickel nanoparticles modified carbon-ceramic electrode. Int J Hydrogen Energy 2011;36:1913-1923.

[40] Qiu R, Zhang XL, Qiao R, Li Y, Kim YI, Kang YS. CuNi Dendritic Material: Synthesis, Mechanism Discussion, and Application as Glucose Sensor. Chem Mater 2007;19:4174-4180.

[41] Goranova D, Avdeev G, Rashkov R. Electrodeposition and characterization of Ni-Cu alloys. Surf Coat Technol 2014;240:204-210.

[42] Jovíc VD, Jovíc BM, Pavlovíc MG. Electrodeposition of Ni, Co and Ni-Co alloy powders. Electrochim Acta 2006;51:5468-5477.

[43] Tarrús X, Montiel M, Vallés E, Gomez E. Electrocatalytic oxidation of methanol on CoNi electrodeposited materials. Int J Hydrogen Energy 2014;39:6705-6713.

[44] Danaee I, Jafarian M, Forouzandeh F, Gobal F, Mahjani MG. Electrocatalytic oxidation of methanol on Ni and NiCu alloy modified glassy carbon electrode. Int J Hydrogen Energy 2008;33:4367-4376.

[45] Nasser AM, Motlak B M. Co_xNi_ydecorated graphene as novel, stable and super effective non-precious electro-catalyst for methanol oxidation. Appl Catal B: Environmental 2014;154-155:221-231.

[46] Chen J, Bradhurst DH, Dou SX, Liu HK. Nickel Hydroxide as an Active Material for the Positive Electrode in Rechargeable Alkaline Batteries. J Electrochem Soc 1999;146:3606-3612.

[47] Danaee I, Jafarian M, Forouzandeh F, Gobal F, Mahjani MG. Electrochemical impedance studies of methanol oxidation on GC/Ni and GC/NiCu electrode. Int J Hydrogen Energy 2009;34:859-869.

[48] Stradiotto NR, Toghill KE, Xiao L, Moshar A, Compton RG. The fabrication and characterization of a nickel nanoparticle modified boron doped diamond electrode for electrocatalysisof primary alcohol oxidation. Electroanalysis 2009;21:2627-2633.

[49] Fleischmann M, Korinek K, Pletcher D. The oxidation of organic compounds at a nickel anode in alkaline solution. J Electroanal Chem Interfacial Electrochem 1971;31:39-49.

[50] Fleischmann M, Korinek K, Pletcher D. The kinetics and mechanism of the oxidation of amines and alcohols at oxide-covered nickel, silver, copper, and cobalt electrodes. J Chem Soc Perkin Trans 1972;2:1396-1403.

[51] Alsabet M, Grden M, Jerkiewicz G. Electrochemical Growth of Surface Oxides on Nickel. Part 1: Formation of β-$Ni(OH)_2$ in Relation to the Polarization Potential, Polarization Time, and Temperature. Electrocatalysis 2011;2;317-330.

[52] Alsabet M, Grden M, Jerkiewicz G. Electrochemical Growth of Surface Oxides on Nickel. Part 1: Formation of β-$Ni(OH)_2$ in Relation to the Polarization Potential, Polarization Time, and Temperature. Electrocatalysis (2014) 5:136-147.

[53] Alsabet M, Grden M, Jerkiewicz G. Electrochemical Growth of Surface Oxides on Nickel. Part 3: Formation of β-NiOOH in Relation to the Polarization Potential, Polarization Time, and Temperature. Electrocatalysis 2015;6:60-71.

[54] Le WZ, Liu YQ. Preparation of nano-copper oxide modified glassy carbon electrode by a novel film plating/potential cycling method and its characterization. Sens Actuators, B 2009;141:147-153.

[55] Othman MR, Salimon J. Analysis of ethanol using copper and nickel sheet electrodes by cyclic voltammetry. The Malaysian Journal of Analytical Sciences 2007;11:379-387.

[56] Barakat NA, El-Newehy M, Al-Deyab SS, Kim HY. Cobalt/copper-decorated carbon nanofibers as novel non-precious electrocatalyst for methanol electrooxidation. Nanoscale research letters 2014;9:2-14.

[57] Druska P, Strehblow HH, Golledge S. A surface analytical examination of passive layers on Cu/Ni alloys: Part I. Alkaline solution. Corros Sci 1996;38:835-851.

[58] Luo P, Prabhu SV, Baldwin RP. Constant potential amperometric detection at a copper-based electrode: electrode formation and operation. Anal Chem 1990;62:752-755.

[59] V.L. Oliveira, C. Morais, K. Servat, T.W. Napporn,G. Tremiliosi-Filho, K.B. Kokoh, Studies of the reaction products resulted from glycerolelectrooxidation on Ni-based materials in alkaline medium. Electrochimica Acta 117 (2014) 255– 262

[60] V.L. Oliveira, C. Morais, K. Servat, T.W. Napporn,G. Tremiliosi-Filho, K.B. Kokoh, Glycerol oxidation on nickel based nanocatalysts in alkaline medium-Identification of the reaction products. Journal of Electroanalytical Chemistry 703 (2013) 56–62.

[61] Y. Kwon, M.T.M. Koper, Combining Voltammetry with HPLC: Application toElectro-Oxidation of Glycerol, Anal. Chem. 82 (2010) 5420–5424.

[62] M. Simões, S. Baranton, C. Coutanceau, Electrochemical Valorisation of Glycerol,ChemSusChem 5 (2012) 2106–2124.

[63] A. Behr, J. Eilting, K. Irawadi, J. Leschinski, F. Lindner, Improved utilisation of renewable resources: New important derivatives of glycerol. Green Chem. 2008, 10, 13-30.

[64] Girishkumar G, Vinodgopal K, Prashant VK. Carbon Nanostructures in Portable Fuel Cells: Single-Walled Carbon Nanotube Electrodes for Methanol Oxidation and Oxygen Reduction. J Phys Chem B 2004;108:19960-19966.

[65] Frode S. Electrochemical Oxidation of Methanol and Formic Acid in Fuel Cell Processes Doctoral theses at NTNU, 2005:204.

Legend of Figures and Scheme:

Fig. 1. SEM images of the Ni/CCE (A), Ni-Cu/CCE [B and C (high magnification)] and Ni-Co/CCE (D).

Fig. 2. EDX spectrums of the Ni/CCE (A), Ni-Cu/CCE (B) and Ni-Co/CCE (C).

Fig. 3. XRD patterns of the Ni/CCE (A), Ni-Cu/CCE (B) and Ni-Co/CCE (C).

Fig. 4. Cyclic voltammograms of the Ni/CCE (A), Ni-Cu/CCE (B) and Ni-Co/CCE (C) recorded at 50 mV s^{-1} in 1.0 M NaOH solution.

Fig. 5. Cyclic voltammograms of the Ni/CCE (A), Ni-Cu/CCE (B) and Ni-Co/CCE (C) recorded at 50 mV s^{-1} in absence (black lines) and presence (red lines) of 0.1 M glycerol in 1.0 M NaOH solution.

Fig. 6. Tafel plots from the electrooxidation of 0.1 M glycerol in 1.0 M NaOH solution at scan rate of 20 mV s^{-1} on the Ni/CCE (A), Ni-Cu/CCE (B) and Ni-Co/CCE (C).

Fig. 7. Effect of scan rate on the electrooxidation of 0.1 M glycerol in 1.0 M NaOH at the Ni/CCE (A), Ni-Cu/CCE (B) and Ni-Co/CCE (C). The insets [I, I' and I" respectively for the Ni/CCE (A), Ni-Cu/CCE (B) and Ni-Co/CCE (C)] show the dependence of the forward anodic peak currents on the square root of scan rates and insets [II, II' and II" respectively for the Ni/CCE (A), Ni-Cu/CCE (B) and Ni-Co/CCE (C)] show the dependence potentials of the forward anodic peak on the square root of scan rates.

Fig. 8. Chronoamperometric curves for the electrooxidation of 0.1 M glycerol at the Ni/CCE (A), Ni-Cu/CCE (B) and Ni-Co/CCE (C) in 1.0 M NaOH solution at two applied potentials (0.6 V and 0.8 V) for Ni/CCE, (0.6 V and 0.75 V) for Ni-Cu/CCE and (0.4 V and 0.55 V) for Ni-Co/CCE.

Scheme 1: Schematic diagram for the oxidation of the glycerol and resulted products at the present modified electrodes in alkaline media based on the literature.

Table caption:

Table 1. Electrochemical parameters of glycerol electrooxidation on the present electrocatalysts.

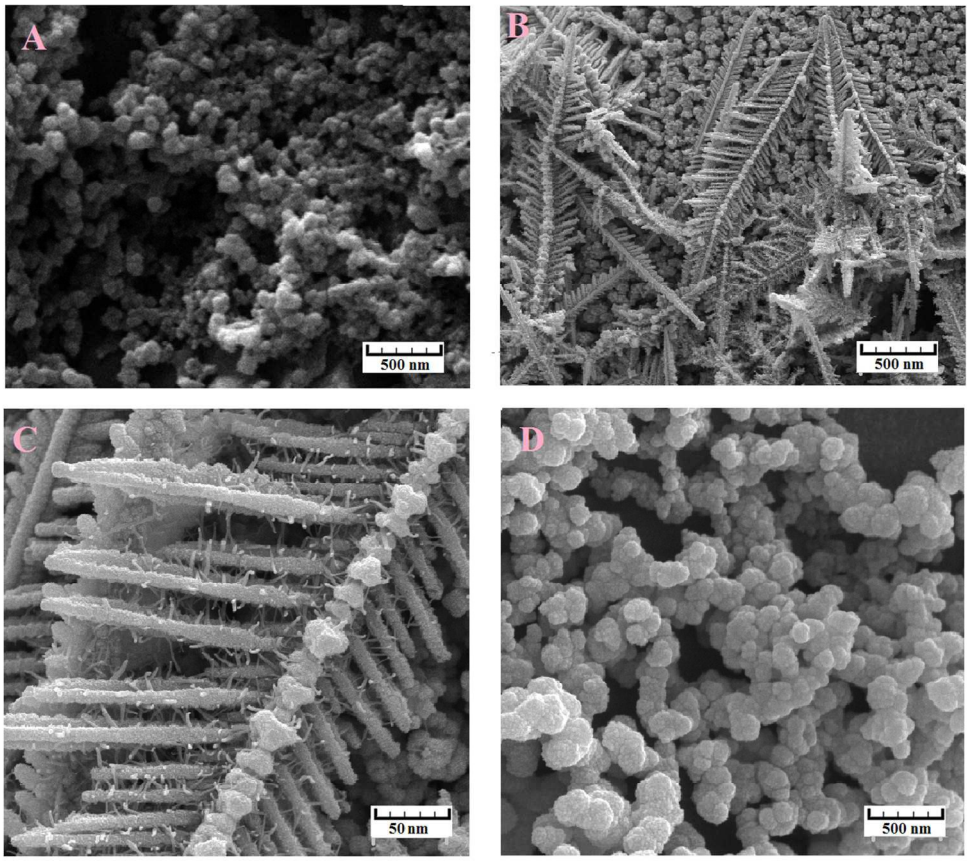

Fig. 1

354x352mm (96 x 96 DPI)

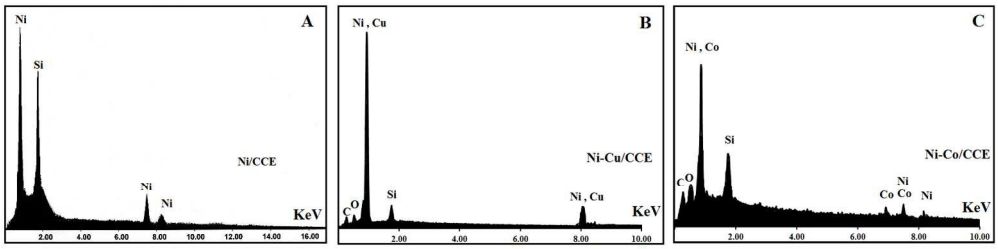

Fig. 2

477x138mm (96 x 96 DPI)

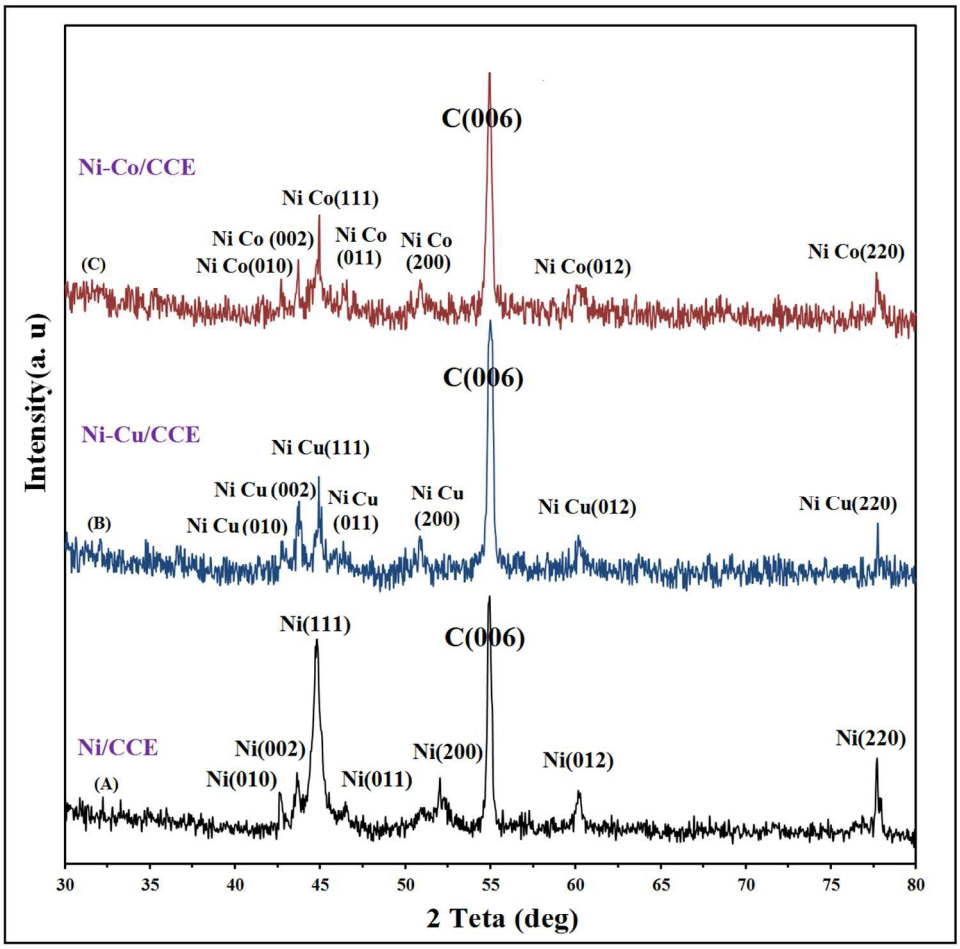

Fig. 3

Fig. 3. XRD patterns of the Ni/CCE (A), Ni-Cu/CCE (B) and Ni-Co/CCE (C).
352x366mm (96 x 96 DPI)

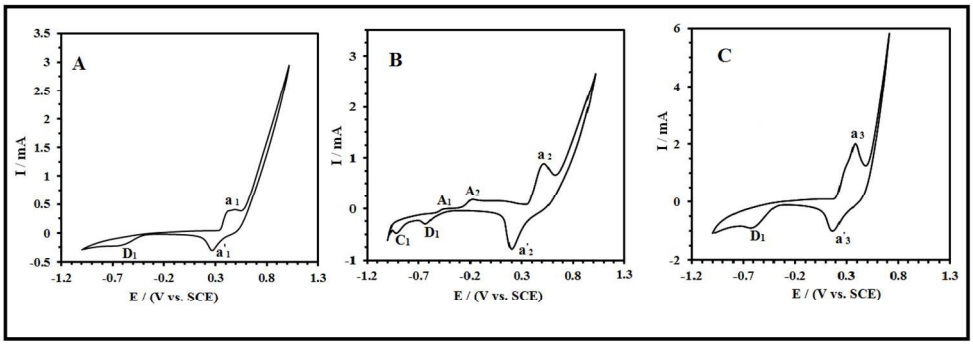

Fig. 4

379x159mm (96 x 96 DPI)

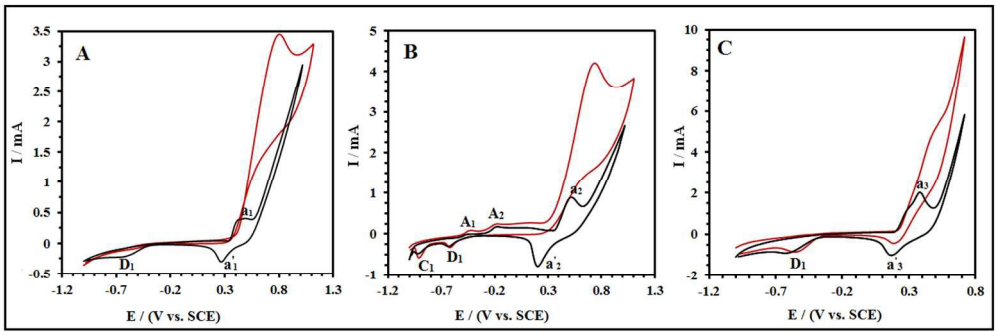

Fig. 5

359x134mm (96 x 96 DPI)

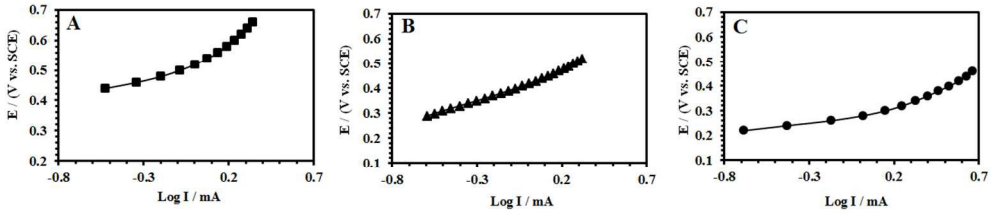

Fig. 6

Fig. 6. Tafel plots from the electrooxidation of 0.1 M glycerol in 1.0 M NaOH solution at scan rate of 20 mV s−1 on the Ni/CCE (A), Ni-Cu/CCE (B) and Ni-Co/CCE (C).
348x110mm (96 x 96 DPI)

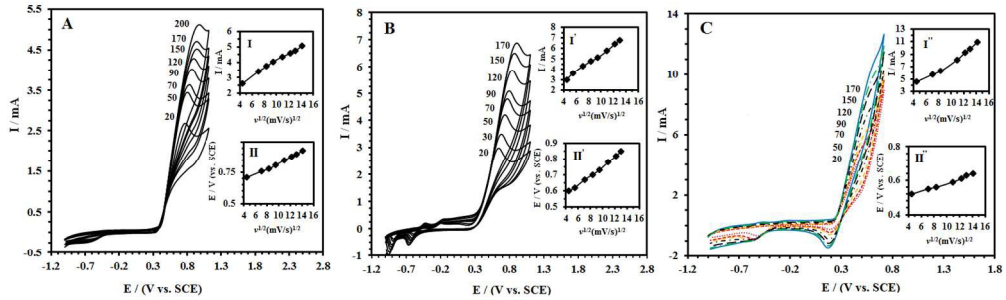

Fig. 7. Effect of scan rate on the electrooxidation of 0.1 M glycerol in 1.0 M NaOH at the Ni/CCE (A), Ni-Cu/CCE (B) and Ni-Co/CCE (C). The insets [I, I' and I" respectively for the Ni/CCE (A), Ni-Cu/CCE (B) and Ni-Co/CCE (C)] show the dependence of the forward anodic peak currents on the square root of scan rates and insets [II, II' and II" respectively for the Ni/CCE (A), Ni-Cu/CCE (B) and Ni-Co/CCE (C)] show the dependence potentials of the forward anodic peak on the square root of scan rates.
431x154mm (96 x 96 DPI)

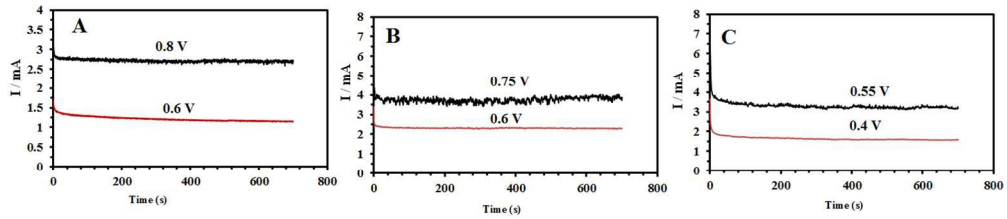

Fig. 8

Fig. 8. Chronoamperometric curves for the electrooxidation of 0.1 M glycerol at the Ni/CCE (A), Ni-Cu/CCE (B) and Ni-Co/CCE (C) in 1.0 M NaOH solution at two applied potentials (0.6 V and 0.8 V) for Ni/CCE, (0.6 V and 0.75 V) for Ni-Cu/CCE and (0.4 V and 0.55 V) for Ni-Co/CCE.
390x108mm (96 x 96 DPI)

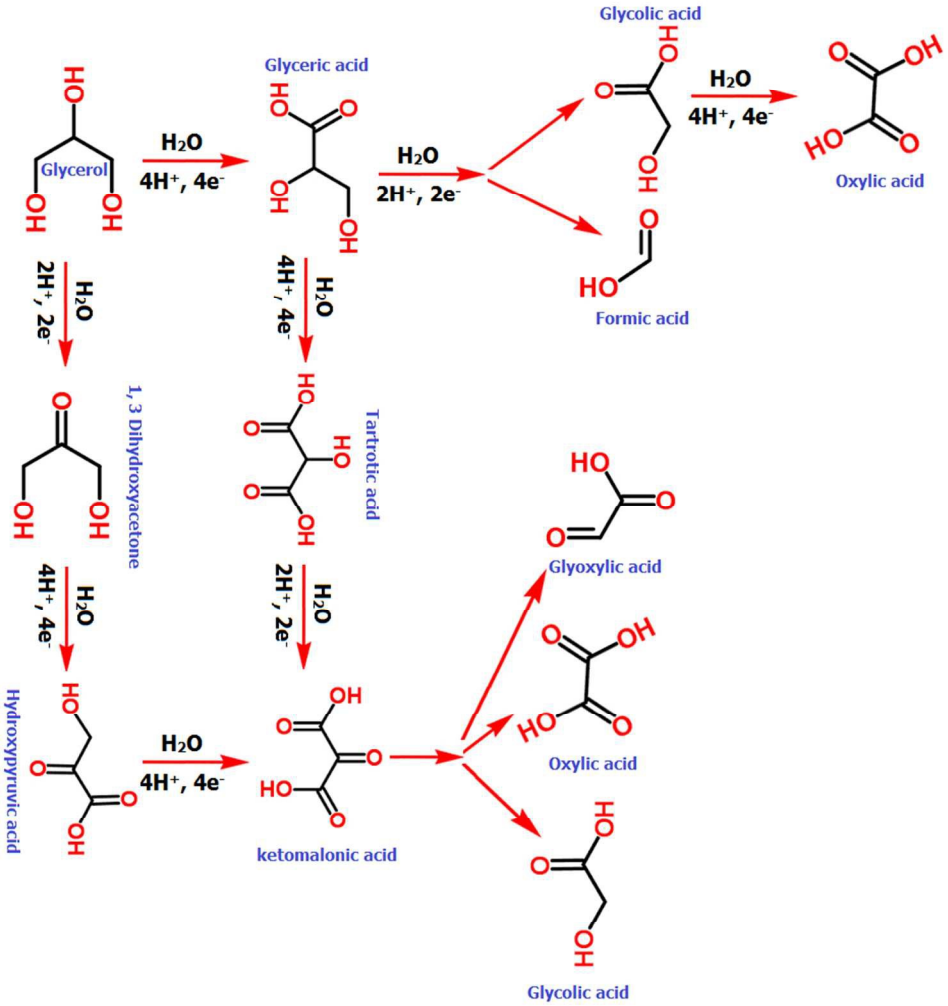

Scheme 1

Scheme 1: Schematic diagram for the oxidation of the glycerol and resulted products at the present modified electrodes in alkaline media based on the literature.
260x297mm (96 x 96 DPI)

Table 1. Electrochemical parameters of glycerol electrooxidation on the present electrocatalysts.

Fuel	Electrocatalyst	E_{Onset} (V)	E_{pf} (V)	I_{pf} (mA)
Glycerol	Ni/CCE	0.40	0.79	3.44
	Ni-Cu/CCE	0.30	0.70	4.12
	Ni-Co/CCE	0.22	0.55	5.74